European Radiology (2022) 32:7883–7895
https://doi.org/10.1007/s00330-022-08826-z

MAGNETIC RESONANCE

Performance of adding hepatobiliary phase image in magnetic resonance imaging for detection of hepatocellular carcinoma: a meta-analysis

Jielin Pan[1,2] · Wenjuan Li[2] · Lingjing Gu[1] · Chaoran Liu[2] · Ke Zhang[2] · Guobin Hong[2]

Received: 8 December 2021 / Revised: 2 March 2022 / Accepted: 20 April 2022 / Published online: 17 May 2022

Abstract

Objectives To determine the performance of diagnostic algorithm of adding hepatobiliary phase (HBP) images in Gd-EOB-DTPA-enhanced MRI for the detection of hepatocellular carcinoma (HCC) measuring up to 3 cm in patients with chronic liver disease.

Methods We searched multiple databases from inception to April 10, 2020, to identify studies on using Gd-EOB-DTPA-enhanced MRI for the diagnostic accuracy of HCC (≤ 3 cm) in patients with chronic liver disease. The diagnostic algorithm of Gd-EOB-DTPA-enhanced MRI with HBP for HCC was defined as a nodule showing hyperintensity during arterial phase and hypointensity during the portal venous, delayed, or hepatobiliary phases. For gadoxetic acid–enhanced MRI without HBP, the diagnostic criteria were a nodule showing arterial enhancement and hypointensity on the portal venous or delayed phases. The data were extracted to calculate summary estimates of sensitivity, specificity, diagnostic odds ratio, likelihood ratio, and summary receiver operating characteristic (sROC) by using a bivariate random-effects model.

Results Twenty-nine studies with 2696 HCC lesions were included. Overall Gd-EOB-DTPA-enhanced MRI with HBP had a sensitivity of 87%, specificity of 92%, and the area under the sROC curve of 95%. The summary sensitivity of Gd-EOB-DTPA-enhanced MRI with HBP was significantly higher than that without HBP (84% vs 68%, $p = 0.01$).

Conclusion Gd-EOB-DTPA-enhanced MRI with HBP showed higher sensitivity than that without HBP and had comparable specificity for diagnosis of HCC in patients with chronic liver disease.

Key Points

- *Hypointensity on HBP is a major feature for diagnosis of HCC.*
- *Extending washout appearance to the transitional or hepatobiliary phase on Gd-EOB-DTPA provides favorable sensitivity and comparable specificity for diagnosis HCC.*
- *The summary sensitivity of gadoxetic acid–enhanced MRI with HBP was significantly higher than that without HBP (84% vs 68%, p = 0.01) for diagnosis of HCC in patients with chronic liver disease.*

Keywords Hepatocellular carcinoma · Gadoxetic acid · Magnetic resonance imaging · Diagnostic performance · Meta-analysis

Abbreviations

AASLD	The American Association for the Study of Liver Diseases
AUC	Area under the summary receiver operating characteristic curve
CI	Confidence interval
DOR	Diagnostic odds ratios
FN	False-negative
FP	False-positive
Gd-EOB-DTPA	Gadoxetic acid
HBP	Hepatobiliary phase
HCC	Hepatocellular carcinoma

Jielin Pan, Wenjuan Li and Lingjing Gu contributed equally to this work.

✉ Guobin Hong
honggb@mail.sysu.edu.cn

[1] Department of Radiology, Zhuhai People's Hospital, Zhuhai Hospital affiliated with Jinan University, Zhuhai 519000, China

[2] Department of Radiology, the Fifth Affiliated Hospital, Sun Yat-Sen University, Zhuhai 519000, China

MRI	Magnetic resonance imaging
NLR	Negative likelihood ratio
PLR	Positive likelihood ratio
sROC	Summary receiver operating characteristic
TN	True-negative
TP	True-positive

Introduction

Hepatocellular carcinoma (HCC) is the sixth most prevalent cancer and the third most frequent cause of cancer-related death worldwide [1–3]. Patient prognosis can achieve a 5-year survival rate of higher than 50% if the HCC is diagnosed at an early stage; especially those within Milano criteria (up to three nodules ≤ 3 cm) may be curable and have a desirable prognosis [2]. More accurate detection of HCC at the early stage (≤ 3 nodules ≤ 3 cm each patient) may reduce the risk of tumor recurrence [4, 5]. Therefore, it is important to effectively improve the sensitivity of diagnosis for HCC at the early stage. HCC can be diagnosed by dynamic contrast-enhanced MRI based on typical imaging feature, hyperintensity on arterial phase, and hypointenstity on portal venous or delayed phases [6, 7]. However, there are still some challenges in the detection and characterization of small HCC because lacking typical imaging feature may lead to lower sensitive (44–62%) for small HCC [8], failing to identify approximately 40% small HCC cases [9, 10].

The introduction of liver-specific contrast agent gadoxetic acid (Gd-EOB-DTPA) provides both hemodynamic information during early dynamic phases and additional information during the hepatobiliary phase (HBP) [11–14]. Most HCC displays hypointensity on HBP, and this feature weights differently depending on the guidelines. Hypointensity on HBP is a major feature in Asian guidelines, whereas western guideline considers it to be an ancillary feature, not sufficient to make a conclusive diagnosis of HCC because of concern over the loss of specificity [7, 15, 16]. Many studies have shown that the combined interpretation of dynamic phase and hypointensity on HBP images improves the diagnostic accuracy of Gd-EOB-DTPA-enhanced MRI for detection of HCC [13, 17–22]. As a consequence, hypointensity on the HBP may be a major hallmark to detect small HCC for Gd-EOB-DTPA-enhanced MRI, particularly for atypical nodules with arterial enhancement but no portal venous or delayed phase washout.

The purpose of our study was to perform a meta-analysis to synthesize the diagnostic accuracy of combining HBP with dynamic phase in gadoxetic acid–enhanced MRI for detection of HCC measuring up to 3 cm, and compare with contrast-enhanced MRI without HBP images based on hyperintense on arterial phase followed by venous or delayed phases washout in patients with chronic liver disease. We also explored factors that may influence the diagnostic accuracies for HCC of enhanced MRI.

Materials and methods

This meta-analysis was performed according to the Preferred Reporting Items for Systematic Reviews and Meta-Analyses for diagnostic test accuracy study (PRISMA-DTA) [23].

Search strategy

Literature search was performed in several databases, including PubMed, Web of Science, Embase, and Scopus, to retrieve studies about gadoxetic acid–enhanced MRI published from inception to April 10, 2020. The comprehensive search strategy was as the following terms: hepatocellular carcinoma/HCC, MRI/magnetic resonance imaging, and gadoxetic/gadoxetate/EOB/eovist/primovist. We excluded review article, abstracts, case reports, letters, and comments. All potentially appropriate studies were retrieved for full-text assessment.

Study selection

Two radiologists (with 5 and 7 years of experience in radiology, respectively) evaluated the titles and abstracts, respectively. Disagreements between the two reviewers were resolved by face-to-face discussion. The eligible full-text articles were retrieved and evaluated by the same two reviewers.

Studies were included when they met all of the following criteria: (1) study population older than 18 years with chronic liver disease and hepatic nodules; (2) suspected HCC; (3) diagnostic accuracy of Gd-EOB-DTPA-enhanced MRI; (4) histopathologic examinations (including biopsy, resection, explant), transcatheter arterial chemoembolization, or clinical follow-up period of at least 6 months as the reference standard; and (5) articles written in English. Studies were excluded when they met at least one of the following criteria: (1) all nodules with a diameter larger than 3 cm; (2) not original research, such as reviews, meta-analysis, letters or meeting abstracts; (3) articles without HBP; (4) data not available to extract or calculate true-positive (TP), false-positive (FP), false-negative (FN), or true-negative (TN); or (5) sample size fewer than 10 lesions. Disagreements of included studies between the two reviewers were resolved by discussion with a third radiologist with 20 years of experience in radiology.

Data extraction

Two previously mentioned reviewers independently screened and extracted the relevant data (TP, FP, TN, FN) from the included studies for meta-analysis.

We recorded the following basic information of each study: primary author, year of publication, type of journal, country, type of study design (retrospective or prospective study), number of patients, number of males and females, range of age and mean age, cause of cirrhosis, lesion number, size range of lesions, and reference standard, the magnetic field strength, rate of Gd-EOB-DTPA injection, acquiring time of arterial phase, portal venous phase, delayed phase and hepatobiliary phase, section thickness of contrast-enhanced imaging, and intensity in HBP of each lesion (Table 1).

The diagnostic algorithm of Gd-EOB-DTPA-enhanced MRI with HBP for HCC was defined as a nodule showing hyperintensity in arterial phase and hypointensity in the portal venous, delayed, or hepatobiliary phases. Without HBP, the diagnostic criteria of enhanced MRI were a nodule showing hyperintensity in arterial phase and hypointensity in the portal venous or delayed phases. Data (TP, FP, FN, TN values) for the detection of up to 3 cm nodules of enhanced MRI were extracted or calculated to reconstruct a 2 × 2 contingency table. If a study reported diagnostic accuracy data of multiple observers, we chose data of the most experienced observer.

Methodological quality and risk of bias assessment

The Quality Assessment of Diagnostic Accuracy Studies 2 (QUADAS-2) [24] was used to evaluate the risk of bias on the study level (Supporting Figure S1).

Statistical analysis

Data extracted from included studies were divided into set 1 and set 2. The data of set 1 consisted of studies containing extractable data for Gd-EOB-DTPA-enhanced MRI with HBP. The data of set 2 were composed of studies containing extractable data for enhanced MRI without HBP.

Data for Gd-EOB-DTPA-enhanced MRI with HBP For several studies involving exact data of TP, FP, FN, and TN from set 1, the following parameters were calculated by using a bivariate random-effects model: sensitivity, specificity, positive likelihood ratio (PLR), negative likelihood ratio (NLR), and diagnostic odds ratios (DOR). All corresponding 95% confidence intervals (CIs) were calculated. A summary receiver operating characteristic (sROC) curve and the area under the sROC curve (AUC) with relevant 95% CIs were also generated. All the studies from set 1 were only combined to calculate sensitivity due to the absence of true-negative data in several studies from this set.

Data for enhanced MRI without HBP Due to the absence of exact true-negative data for enhanced MRI without HBP in studies from set 2, only the sensitivities of set 2 studies were combined and calculated.

Subgroup analysis Subgroup analysis was based on factors that potentially affected diagnostic sensitivity or caused heterogeneity. More details of potential factors about subgroup analysis are provided in Table 2.

The z test was used to compare the summarized sensitivity between enhanced MRI with HBP and without HBP. Heterogeneity was quantified by Q and I^2 [25]. The MIDAS model [26] was used to perform the bivariate random-effects model and generate the sROC curve. $p < 0.05$ indicate a statistically significant difference. Funnel plots were used to assess the publication bias. More detailed description of the statistical methods can be found in the supplementary materials [27, 28].

Results

Study selection

Finally, 29 studies and 3554 lesions (HCC = 2696) were included in the meta-analysis (Fig. 1). Seventeen studies reported comprehensive parameters for the diagnostic accuracy, while the other 12 studies reported only sensitivity. Among the 29 studies (*group 1*, 17 studies containing extractable data both for MRI with HBP and without HBP; *group 2*, 7 studies only containing extractable data for MRI with HBP; and *group 3*, 5 studies only containing extractable data for MRI without HBP), studies of *group 1* plus *group 2* constituted set 1 and studies of *group 1* plus *group 3* constituted set 2 (Table 1).

Characteristics of studies

Characteristics of the 29 included studies are summarized in Table 1. All included studies used a single-center design. In the 17 studies [17, 21, 22, 29–42], data could be extracted to calculate the TP, FP, FN, and TN values for Gd-EOB-DTPA-enhanced MRI with HBP. In the remaining 12 studies [18, 43–53], only the data of sensitivity could be extracted. The size of the lesions was ranging from 2 to 30 mm for Gd-EOB-DTPA-enhanced MRI. Seven studies used a prospective design, and the other 22 used a retrospective design. Magnetic field strength was 3.0 T in thirteen studies, lower than 3.0 T in 12 studies, a combination of 3.0 T and 1.5 T in 3 studies [35, 37, 44], and one study was unclear [21]. Contrast agent injection was administered at a rate of 2 ml/s in 9 studies, slower than 2 ml/s in 19 studies, and remaining one study was unclear [21]. After contrast agent administration, enhanced MRI of early and late arterial phases were performed with a threshold of 20 s. Nine studies performed enhanced MRI in the early arterial phase, whereas 18 studies performed late arterial phase. Two remaining study lacked a concrete value about acquisition time of the arterial phase [21, 48]. The

Table 1 Characteristics of Gd-EOB-DTPA-enhanced MRI of included studies

Study and publication year	Study design/ country	Magnetic field strength (T)	Patients	Age (years)	Etiology of cirrhosis	Reference standard	No. of lesions	No. of HCC lesions	Nodule size (mm)	Contrast injection rate (ml/s)	Time of acquiring arterial phase (s)
*Group 1**											
Golfieri R. et al, 2011 [34]	Prospective/Italy	1.5	127	54 (31–77)	HBV = 44, HCV = 65, alcoholic = 18	HP = 215	215	173	16 (4–20)	2	7
Granito A. et al, 2013 [33]	Prospective/Italy	1.5	33	70 (48–84)	HBV = 6, HCV = 19, alcoholic = 1, cryptogenic = 4, NASH = 2, PBC = 1	HP = 13, follow-up at least 22 months = 15, TVP = 24	48	38	18 (10–30)	1	10
Di Pietropaolo M. et al, 2015 [30]	Retrospective/Italy	1.5	41	70 (50–85)	HBV = 11, HCV = 23, alcoholic = 1, PBC = 1, cryptogenic = 3	HP, TVP, follow-up at least 24 months (absolute value NA)	87	68	(4–28)	0.8–1	30–35
Choi S.H. et al, 2016 [29]	Retrospective/South Korea	1.5	198	58.1 ± 9.8	HBV = 167, HCV = 12, alcoholic = 10, cryptogenic = 9	HP = 184, follow-up at least 24 months = 79, TACE/RAF = 32	295	194	18.2 (10–30)	1	5
Kim Y.K. et al, 2010 [18]	Prospective/South Korea	1.5	41	(40–74)	HBV = 38, HCV = 3	HP = 25, TACE = 31	56	56	15 (5–20)	1	20
Yu M.H. et al, 2014 [44]	Retrospective/South Korea	1.5 or 3.0	60	60.1 (40–78)	NA	HP = 42, TACE = 34	76	76	7.1 (2–10)	1 or 1.5	7
Rhee H. et al, 2012 [48]	Retrospective/South Korea	3.0	15	56 (30–67)	HBV = 12, HCV = 1, alcoholic = 1, MPF = 1	HP = 19	19	19	15 (4–30)	2	NA
Kawada N. et al, 2010 [52]	Retrospective/Japan	3.0	13	67 (51–77)	HBV = 1, HCV = 8, alcoholic = 1, cryptogenic = 3	HP = 15	15	15	(< 20)	2	20
Paisant A. et al, 2020 [35]	Prospective/France	1.5 or 3.0	171	66.2 ± 8.9	HBV = 14, HCV = 47, alcoholic = 105 Others = 59	HP = 137, follow-up at least 6 months = 88	225	153	17.3 (10–30)	1	7–8
Zhou Y. et al, 2019 [36]	Retrospective/China	3.0	98	55.9 ± 8.6	HBV = 84, HCV = 14	HP = 99, follow-up at least 6 months = 17	116	89	15.7 (≤ 20)	1	15–18
Kim D. H. et al, 2019 [22]	Retrospective/South Korea	1.5	178	55.3 ± 9.1	HBV=155, HCV = 5, HBV+HCV = 2, alcoholic = 10 Others = 6	HP = 203	203	186	19.8 (10–30)	1	5
Renzulli M. et al, 2018 [21]	Retrospective/Italy	NA	228	63.7 ± 10.6	HBV = 22, HCV = 114, alcoholic = 45 Others = 47	HP and follow-up	279	224	≤ 20	NA	NA
Joo I. et al, 2015 [37]	Retrospective/South Korea	1.5 or 3.0	NA	NA	NA	HP = 167	167	97	≤ 20	1.5	7
Kim Y. K. et al, 2014 [38]	Retrospective/South Korea	3.0	157	57 (30–76)	HBV = 140, HCV = 11, Others = 6	HP = 182	182	136	≤ 20	1	20–35
Kim M. Y. et al, 2013 [39]	Retrospective/South Korea	3.0	176	59 (45–72)	NA	HP = 191	191	181	18 (6–30)	1	20–35
		3.0	189	63	HBV = 171, HCV = 18		240	240	≤ 30	1	20–35

Table 1 (continued)

Study and publication year	Study design/ country	Magnetic field strength (T)	Patients	Age (years)	Etiology of cirrhosis	Reference standard	No. of lesions	No. of HCC lesions	Nodule size (mm)	Contrast injection rate (ml/s)	Time of acquiring arterial phase (s)
Kim A. Y. et al, 2012 [50]	Retrospective/South Korea			(27–79)		HP = 132, clinical and radiologic findings = 57					
Chou C. T. et al, 2010 [42]	Prospective/China	1.5	NA	NA	NA	HP and follow-up	22	7	≤ 30	2	25–30
*Group 2***											
Zhao X. T. et al, 2014 [31]	Retrospective/China	3.0	33	54 (20–80)	HBV = 27, HCV = 3, alcoholic = 3	HP = 30, TACE = 9, follow-up at least 12 months = 15	54	34	12 (5–20)	1.5	25–30
Park M. J. et al, 2012 [17]	Retrospective/South Korea	3.0	260	55.1 ± 7.9	HBV = 242, HCV = 8	HP = 218, follow-up at least 12 months = 105	323	179	(≤ 20)	1	20–35
Park M. J. et al, 2013 [32]	Retrospective/South Korea	3.0	148	55 (30–73)	HBV = 136 HCV = 12	HP = 125, follow-up at least 11 months = 10	135	102	13 (6–20)	1	20–35
Kim Y. K. et al, 2011 [51]	Prospective/South Korea	1.0	40	63 (45–77)	HBV = 38, HCV = 2	HP = 26, TACE = 28	54	54	15 (6–20)	1	20–30
Hwang J. et al, 2014 [40]	Retrospective/South Korea	3.0	NA	NA	NA	HP = 114	114	68	≤ 20	1	20–35
Ooka Y. et al, 2013 [46]	Retrospective/Japan	1.5	NA	NA	NA	HP = 59	59	55	≤ 20	2	23
Kim Y. K. et al, 2010 [41]	Retrospective/South Korea	1.5	35	(35–76)	NA	HP, TACE and follow-up	67	18	≤ 30	1	20–35
*Group 3****											
Rhee H. et al, 2012 [49]	Retrospective/South Korea	1.5	34	57 (30–66)	HBV = 28, HCV = 1, alcoholic = 4, cryptogenic = 1	HP = 60	60	29	12.9 (3–30)	2	30–35
Choi J. W. et al, 2013 [47]	Retrospective/South Korea	3.0	216	57.2 (22–82)	HBV = 167, HCV = 14, alcoholic = 10, cryptogenic = 25	HP = 97	97	97	(≤ 20)	1.5	7
Park V. Y. et al, 2014 [45]	Retrospective/South Korea	3.0	55	55 (28–73)	HBV = 49, HCV = 3, alcoholic = 1, cryptogenic = 2	HP = 67	67	67	20.2 (≤ 30)	2	20–35
Choi M. H. et al, 2017 [43]	Retrospective/South Korea	3.0	84	58.9 (30–77)	NA	HP = 67	67	67	13.5 (5–19)	2	30–35
Di Martino M. et al, 2010 [53]	Prospective/Italy	1.5	NA	NA	NA	HP and follow-up	75	55	≤ 20	2	20–40

Abbreviations: *Gd-EOB-DTPA*, gadolinium-ethoxybenzyl-diethylenetriamine penta-acetic acid; *MRI*, magnetic resonance imaging; *HBV*, hepatitis B virus; *HCV*, hepatitis C virus; *HP*, histopathologic examination (biopsy; resection; explant); *TACE*, transcatheter arterial chemoembolization; *NASH*, non-alcoholic steatohepatitis; *PBC*, primary biliary cirrhosis; *MPF*, mild perivenular fibrosis; *TVP*, typical vascular pattern; *RFA*, radiofrequency ablation; *NA*, not available. Group 1*, 17 studies containing extractable data both for Gd-EOB-DTPA-enhanced MRI with HBP and without HBP; group 2**, 7 studies only containing extractable data for Gd-EOB-DTPA-enhanced MRI adding HBP; group 3***, 5 studies only containing extractable data for Gd-EOB-DTPA-enhanced MRI without HBP histopathologic examination (biopsy, resection, explant) was the sole reference standard for all lesions in 13 studies, and a combination of histopathology, clinical follow-up, transcatheter arterial chemoembolization, or radiofrequency ablation as the comprehensive reference standard were performed in the remaining 16 studies. Six studies were conducted outside of Asia, and 23 studies were conducted in Asia. There are 10 studies designed as case series, and another 19 studies are designed as case-control.

Quality assessment

The QUADAS-2 questions evaluated for each study are presented in Supporting Figure S1. The quality assessment results for each study are shown in Supporting Table S1 and Fig. 2. Most of the included studies (14 out of 29) were found to be at a high risk of bias for patient selection due to their retrospective design. The risk of bias for the index test was considered to generate from the awareness of clinical information about patients in reviewing MRI. A combination of histopathology and clinical follow-up as the comprehensive reference standard may result in a substantial risk of bias for the reference standard. The combinational reference standard was a considerable factor that may increase the risk of bias for flow and timing.

Overall diagnostic accuracy

Diagnostic accuracy analysis For 17 studies, data of TP, FP, FN, and TN values could be extracted in set 1 for Gd-EOB-DTPA-enhanced MRI with HBP. The summary estimates for the detection of HCC by using Gd-EOB-DTPA-enhanced MRI with HBP showed a sensitivity of 87% (95% CI: 80%, 92%), specificity of 92% (95% CI: 85%, 96%), PLR of 11.5 (95% CI: 5.8, 22.8), NLR of 0.14 (95% CI: 0.09, 0.22), and DOR of 82 (95% CI: 36, 187). Substantial heterogeneity was exhibited by the Q test for sensitivity ($p < 0.001$) and for specificity ($p < 0.001$) (Fig. 3). The summary ROC curve of Gd-EOB-DTPA-enhanced MRI with HBP is shown in Fig. 4, with an area under the curve of 95% (95% CI: 93%, 97%). Summary estimates of the PLR and NLR for Gd-EOB-DTPA-enhanced MRI with HBP are shown in Fig. 5. Because true-negative data could not be extracted for several studies, the diagnostic accuracy of Gd-EOB-DTPA-enhanced MRI without HBP was not able to be summarized. The specificity of those studies in set 2 ranged from 81 to 100%.

Sensitivity analysis Data from set 1 and set 2 were collected for Gd-EOB-DTPA-enhanced MRI with and without HBP to analyze summary sensitivity, respectively. Gd-EOB-DTPA-enhanced MRI with HBP exhibited significantly higher pooled sensitivity than that without HBP (84% [95% CI: 77%, 90%] vs 68% [95% CI: 57%, 77%], $p = 0.01$). Significant heterogeneity was found for the sensitivity of both MRI with and without HBP ($p < 0.001$ for both) (Fig. 6).

Subgroup analysis

Additional sensitivity estimations for different subgroups were performed for factors that potentially affect diagnostic sensitivity (Table 2).

Sensitivity was significantly lower for studies from Asia than studies from outside of Asia (83% vs 85% for MRI with HBP, 63% vs 77% for MRI without HBP). However, no statistically significant difference was found between this subgroup ($p > 0.05$). In our meta-analysis, a case-control study was defined as a study containing both patients with HCC and a control group of subjects with hepatic lesions other than HCC. A case series study was defined as a study only including patients with hepatocellular carcinoma. Sensitivity of case-control study versus case series study in MRI without HBP was 77% and 57%, with $p = 0.03$. For MRI with HBP, there is no statistically significant difference in this subgroup.

Publication bias

The Deeks funnel plot showed a symmetrical appearance. A low likelihood of publication bias was performed for MRI with HBP in diagnostic accuracy analysis ($p = 0.62$, Supporting Figure S2). Low likelihood of publication bias in the sensitivity analysis was also observed for MRI with HBP ($p = 0.62$, Supporting Figure S3) and MRI without HBP ($p = 0.98$, Supporting Figure S4).

Discussion

Our results showed that Gd-EOB-DTPA-enhanced MRI with HBP for diagnosis HCC demonstrated a high sensitivity of 87% and a specificity of 92%. In a recent meta-analysis, Kierans et al demonstrated the performance of dynamic contrast material-enhanced MRI in the diagnosis of small (≤ 2 cm) HCC based on current guidelines as arterial enhancement and washout [54]. In that meta-analysis, a pooled sensitivity of 87% for MRI with HBP was reported in subgroup analysis, which was higher than those without HBP (pooled sensitivity of 65%). However, the imaging diagnostic criteria of their study were not unified due to some original research referring to DWI in diagnosing HCC. Our meta-analysis clearly defined the diagnostic algorithm and calculated relevant data from the original studies. Compared with extracellular contrast agent MRI, lower depiction of arterial hyperintensity due to the smaller amount of gadolinium injected and problem of pseudowashout for hepatic nodules may appear on Gd-EOB-DPTA MRI. But in our study, extending washout appearance to the transitional or hepatobiliary phase reached a favorable

Table 2 Sensitivity estimates for subgroups analyses of gadoxetic acid–enhanced MRI with and without HBP in detection of small HCC

Subgroup	Pooled sensitivity for MRI with HBP (%)	*p* value	Pooled sensitivity for MRI without HBP (%)	*p* value
Type of study design		0.19		0.26
Prospective study (*n* = 7) [18, 33–35, 42, 51, 53]	90 (78, 96)		76 (63, 85)	
Retrospective study (*n* = 22) [17, 21, 22, 29–32, 36–41, 43–50, 52]	83 (75, 88)		66 (53, 78)	
Magnetic field strength (T)		0.24		0.47
< 3.0 T (*n* = 12) [18, 22, 29, 30, 33, 34, 41, 42, 46, 49, 51, 53]	88 (76, 94)		75 (56, 87)	
3.0 T (*n* = 13) [17, 31, 32, 36, 38–40, 43, 45, 47, 48, 50, 52]	79 (65, 89)		66 (48, 80)	
Injection rate of contrast agent		0.71		0.05
= 2 ml/s (*n* = 9) [34, 42, 43, 45, 46, 48, 49, 52, 53]	77 (25, 96)		49 (26, 73)	
< 2 ml/s (*n* = 19) [17, 18, 22, 29–33, 35–40, 44, 46, 47, 50, 51]	85 (79, 88)		75 (67, 82)	
Acquisition time of AP after injecting contrast agent		0.45		0.26
< 20 s (*n* = 9) [22, 29, 33–37, 44, 47]	86 (75, 93)		75 (63, 84)	
≥ 20s (*n* = 18) [17, 18, 30–32, 38–43, 45, 46, 49–53]	82 (74, 88)		63 (45, 78)	
Reference standard		0.75		0.98
Histopathology as the sole reference standard in all patients (*n* = 13) [22, 34, 37–40, 43, 45–49, 52]	83 (65, 95)		68 (46, 84)	
Histopathology not the reference standard in all patients (*n* = 16) [17, 18, 21, 29–33, 35, 36, 41, 42, 44, 50, 51, 53]	83 (77, 88)		68 (60, 76)	
Country of origin		0.80		0.10
In Asia (*n* = 23) [17, 18, 22, 29, 31, 32, 36–52]	83 (74, 89)		63 (47, 77)	
Outside Asia (*n* = 6) [21, 30, 33–35, 53]	85 (63, 95)		77 (69, 83)	
Case-control or case series studies		0.29		0.03
Case-control studies (*n* = 19) [17, 21, 22, 29–42, 49, 53]	85 (79, 90)		77 (67, 86)	
Case series studies (*n* = 10) [18, 43–48, 50–52]	75 (53, 89)		57 (42, 72)	

In the column of subgroup, the superscript numbers in the parentheses represent corresponding references

Numbers in parentheses are 95% CIs

sensitivity. The diagnostic algorithm for Gd-EOB-DTPA-enhanced MRI with HBP had a significantly higher sensitivity than enhanced MRI without HBP (84% vs 68%, $p = 0.01$) for diagnosis of HCC. The summarized sensitivity of MRI with HBP images for evaluating HCC in any size was 84% in the meta-analysis by Lee et al [55]. In this meta-analysis, they did not evaluate the sensitivity of MRI with HBP images by lesion size or indicate the diagnostic algorithm in the subgroup. Lesion size is an important index in surveillance, diagnostic algorithm, and decisions regarding liver transplantation for hepatocellular carcinoma [7, 56].

Nonhepatocellular tumors also appear hypointense on HBP due to lacking of the organic anion transporting polypeptide, which may reduce the specificity for diagnosing HCC. Excluding benign lesions or non-HCC malignancies will maintain a relatively similar specificity for Gd-EOB-DTPA-enhanced MRI. Our meta-analysis reached a pooled specificity of 92%. The explanation may be that non-HCC malignancies are less frequently encountered in patients with chronic liver disease. Consistent with our meta-analysis, many studies have demonstrated that the addition of HBP in Gd-EOB-DTPA-enhanced MRI allowed higher sensitivity and without a significant reduction in specificity for diagnosis on HCC in patients with chronic liver disease [19, 21, 22, 29, 35, 37, 57, 58].

Subgroup analysis showed that case-control studies demonstrated higher sensitivity than case series studies (77% versus 57%, $p = 0.03$). A possible explanation for these results is that most of the case series studies were small sample size and included lesions smaller than 1 cm only. The classification of

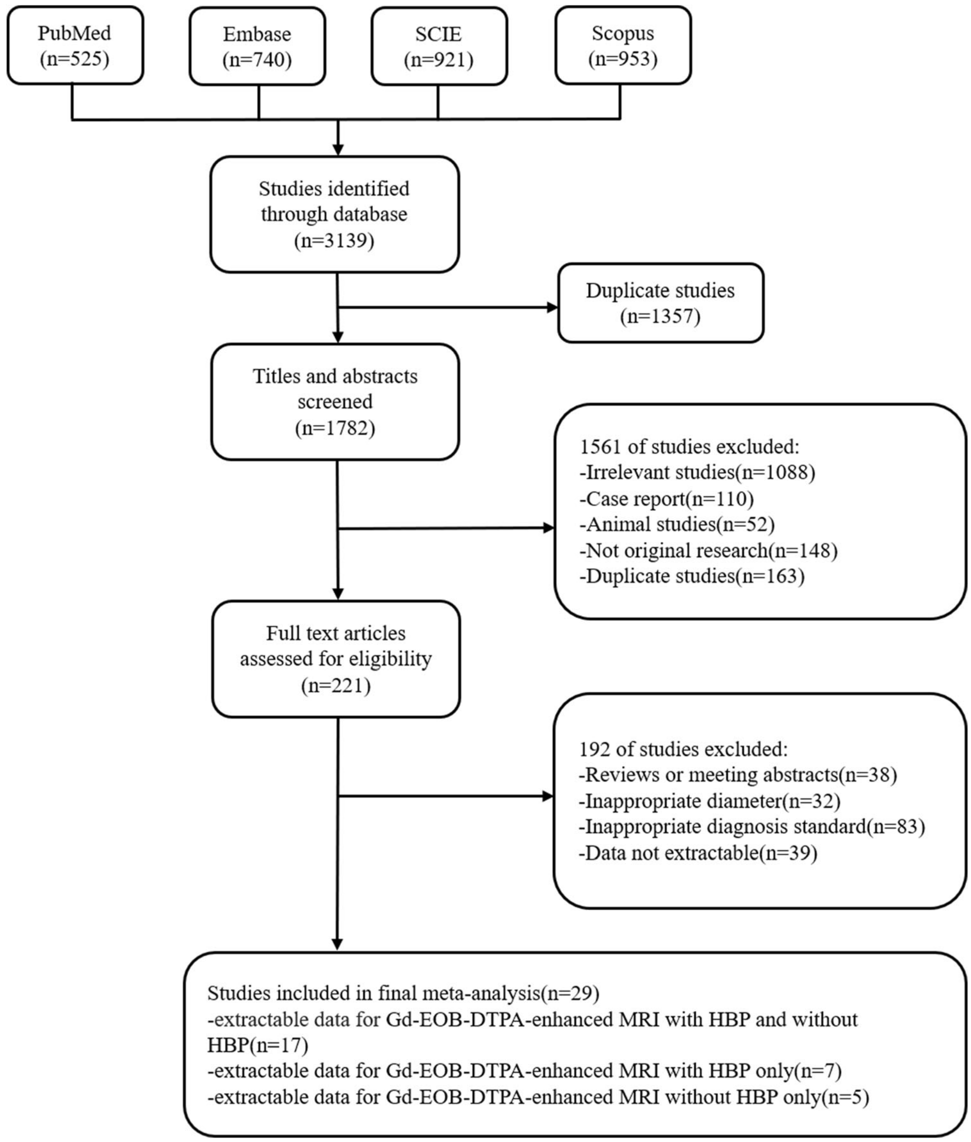

Fig. 1 Studies excluded and included in the study

patients using Child-Pugh may be another potential factor contributing to heterogeneity. However, it was insufficient to obtain relative information from original studies, and the sample was too small for subgroup analysis. Large sample and

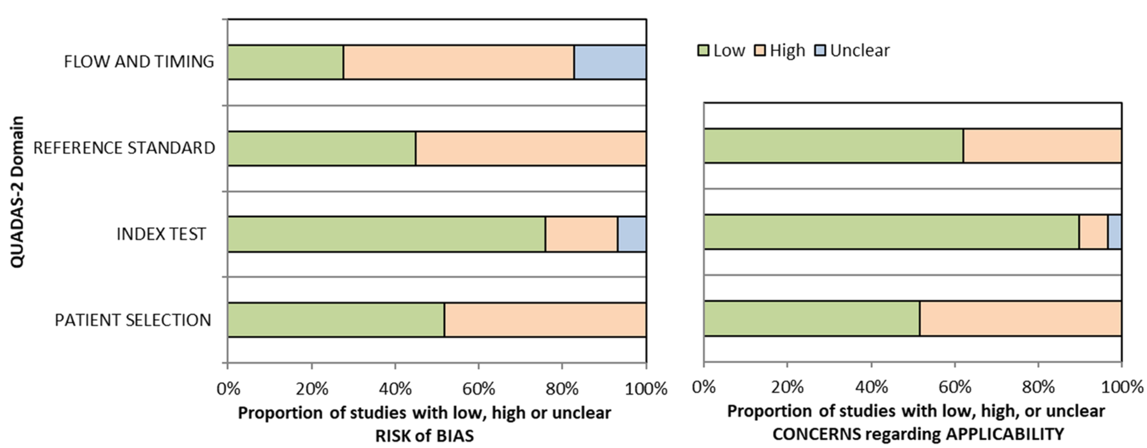

Fig. 2 Quality assessment results for each study

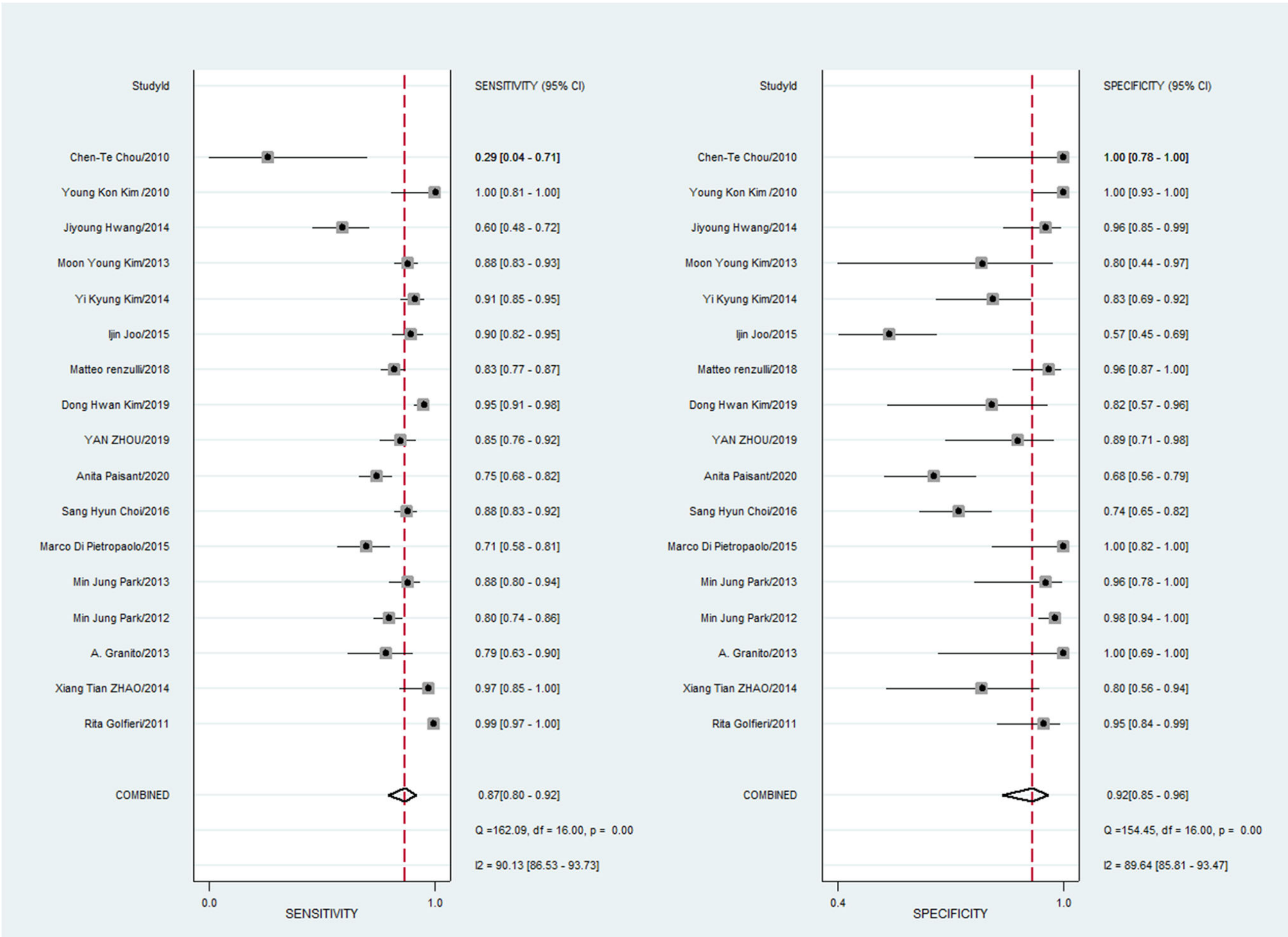

Fig. 3 Summary estimates for the detection of HCC by using Gd-EOB-DTPA-enhanced MRI with HBP

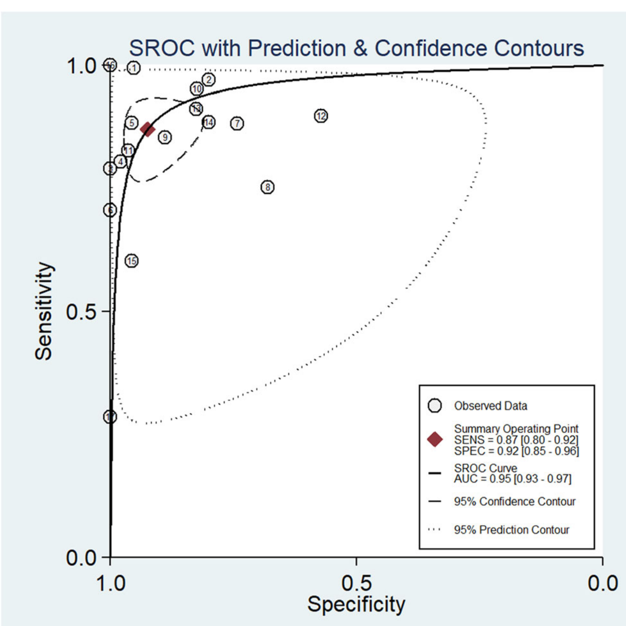

Fig. 4 Summary ROC curve of Gd-EOB-DTPA-enhanced MRI with HBP

high-quality studies are needed to verify this assumption. It is crucial that future studies adopt study designs that can better control biases and provide higher levels of evidence such as cohort studies and randomized controlled trials.

Our meta-analysis has several limitations. First, all the included studies were significantly heterogeneous, which affected the applicability of the summary estimate for diagnosis performance. However, this heterogeneity was useful for the subgroup analysis and may be a factor associated with improving sensitivity of MRI for detecting HCC. Besides, we used random-effects model and the summary ROC model to overcome the heterogeneity. The 95% CIs of sensitivity and specificity were not substantially wide, which demonstrates these results are valuable. Second, only 7 prospective studies were included in our analysis. This may cause a methodological limitation of including a relatively large number of retrospective studies. Pooling such suboptimal retrospective results may have caused a bias toward increased diagnostic sensitivity [59]. Third, we only analyzed the hepatobiliary agent of Gd-EOB-DTPA. Diagnosis performance of other hepatobiliary agents needs to be further analyzed in the future. Finally, our meta-analysis only included studies published in English,

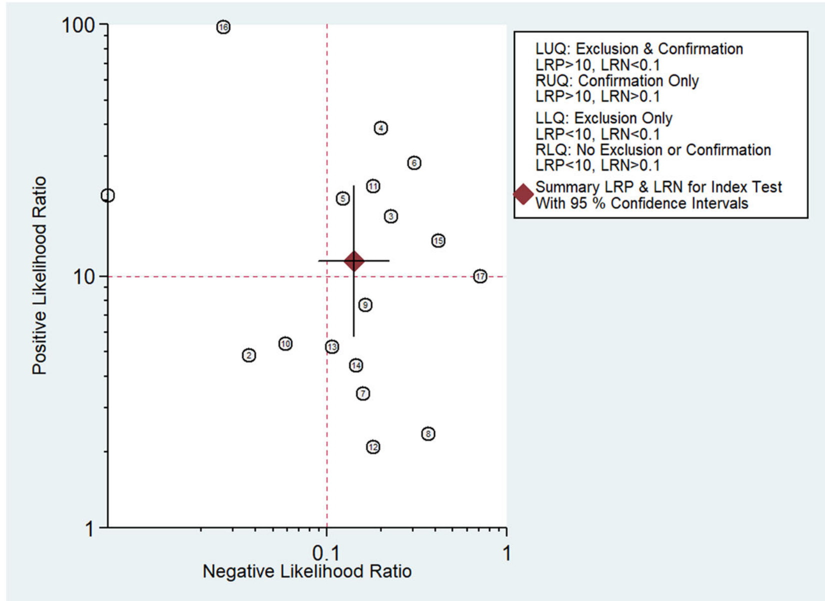

Fig. 5 Summary estimates of the PLR and NLR for Gd-EOB-DTPA-enhanced MRI with HBP

which possibly leads to "Tower of Babel" bias [60]. This bias refers to the possible tendency of investigators speaking non-English to only publish studies with positive results in international journals.

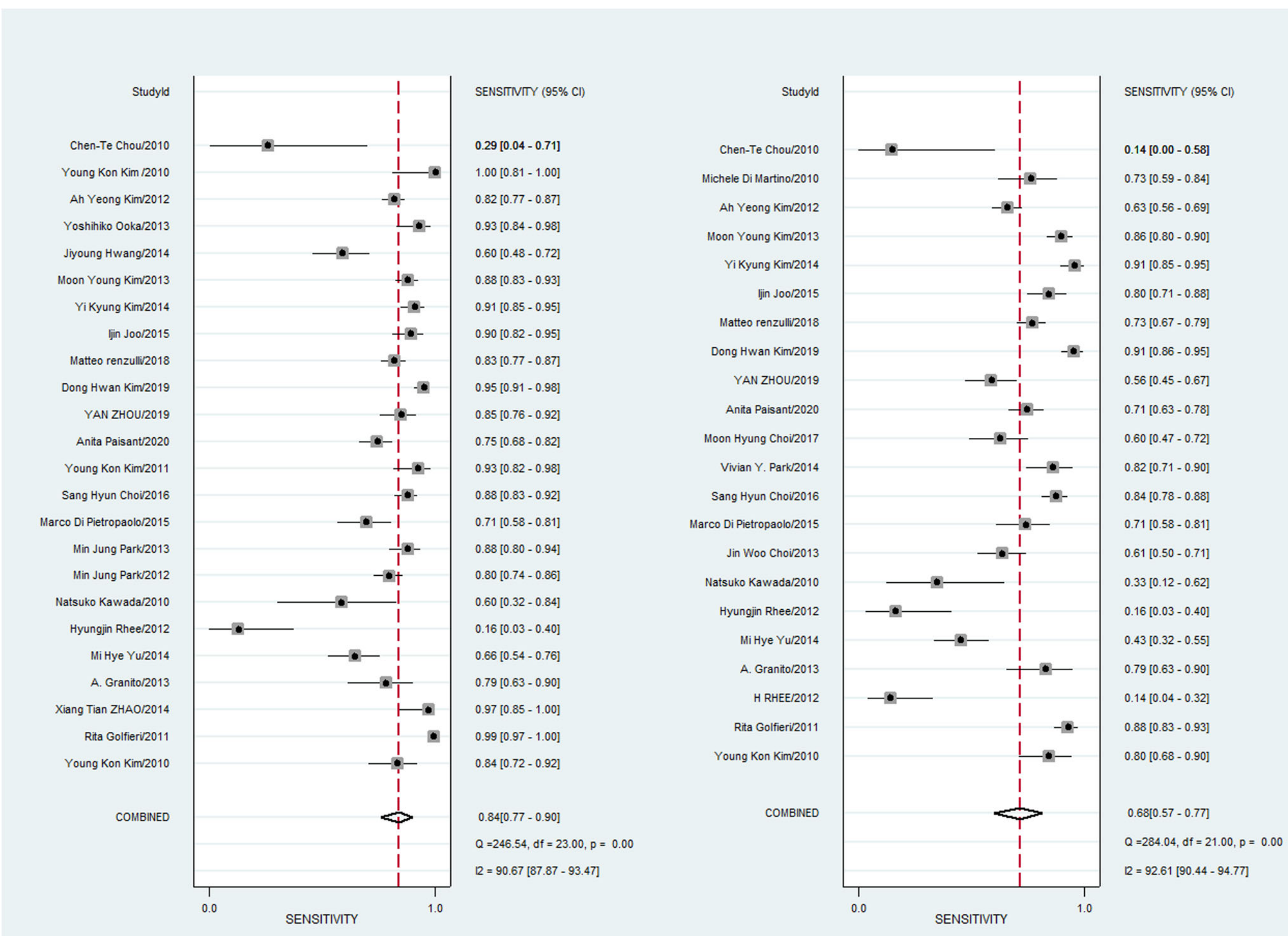

Fig. 6 Summary sensitivities for Gd-EOB-DTPA-enhanced MRI with and without HBP

In conclusion, the results of our meta-analysis suggest that Gd-EOB-DTPA-enhanced MRI with HBP images has significantly higher sensitivity and comparable specificity than enhanced MRI without HBP images for diagnosis of HCC measuring up to 3 cm in patients with chronic liver disease. Therefore, the addition of HBP images in Gd-EOB-DTPA-enhanced MRI should be regarded as a major imaging feature for diagnosis HCC measuring up to 3 cm in patients with chronic liver disease.

Supplementary Information The online version contains supplementary material available at https://doi.org/10.1007/s00330-022-08826-z.

Funding The authors state that this work has not received any funding.

Declarations

Guarantor The scientific guarantor of this publication is Guobin Hong.

Conflict of interest The authors of this manuscript declare no relationships with any companies whose products or services may be related to the subject matter of the article.

Statistics and biometry No complex statistical methods were necessary for this paper.

Informed consent Written informed consent was waived by the Institutional Review Board.

Ethics approval Institutional Review Board approval was obtained.

Methodology
• retrospective
• diagnostic or prognostic study
• multicenter study

References

1. Global Burden of Disease Cancer Collaboration, Fitzmaurice C, Dicker D et al (2015) The global burden of cancer 2013. JAMA Oncol 1:505–527
2. Forner A, Llovet JM, Bruix J (2012) Hepatocellular carcinoma. The Lancet 379:1245–1255
3. Ferlay J, Shin HR, Bray F, Forman D, Mathers C, Parkin DM (2010) Estimates of worldwide burden of cancer in 2008: GLOBOCAN 2008. Int J Cancer 127:2893–2917
4. Soong RS, Yu MC, Chan KM et al (2011) Analysis of the recurrence risk factors for the patients with hepatocellular carcinoma meeting University of California San Francisco criteria after curative hepatectomy. World J Surg Oncol 9:9
5. Imamura H, Matsuyama Y, Tanaka E et al (2003) Risk factors contributing to early and late phase intrahepatic recurrence of hepatocellular carcinoma after hepatectomy. J Hepatol 38:200–207
6. Bruix J, Sherman M, American Association for the Study of Liver Disease (2011) Management of hepatocellular carcinoma: an update. Hepatology 53:1020–1022
7. Marrero JA, Kulik LM, Sirlin CB et al (2018) Diagnosis, staging, and management of hepatocellular carcinoma: 2018 practice guidance by the American Association for the Study of Liver Diseases. Hepatology 68:723–750
8. Zech CJ, Bartolozzi C, Bioulac-Sage P et al (2013) Consensus report of the Fifth International Forum for Liver MRI. AJR Am J Roentgenol 201:97–107
9. Forner A, Vilana R, Ayuso C et al (2008) Diagnosis of hepatic nodules 20 mm or smaller in cirrhosis: prospective validation of the noninvasive diagnostic criteria for hepatocellular carcinoma. Hepatology 47:97–104
10. Bolondi L, Gaiani S, Celli N et al (2005) Characterization of small nodules in cirrhosis by assessment of vascularity: the problem of hypovascular hepatocellular carcinoma. Hepatology 42:27–34
11. Hwang J, Kim YK, Jeong WK, Choi D, Rhim H, Lee WJ (2015) Nonhypervascular hypointense nodules at gadoxetic acid– enhanced Mr imaging in chronic liver disease: diffusion-weighted imaging for characterization. Radiology
12. Van Beers BE, Pastor CM, Hussain HK (2012) Primovist, Eovist: what to expect? J Hepatol 57:421–429
13. Ahn SS, Kim MJ, Lim JS, Hong HS, Chung YE, Choi JY (2010) Added value of gadoxetic acid– enhanced hepatobiliary phase MR imaging in the diagnosis of hepatocellular carcinoma. Radiology 255:459–466
14. Choi JY, Lee JM, Sirlin CB (2014) CT and MR imaging diagnosis and staging of hepatocellular carcinoma. Part II. Extracellular agents, hepatobiliary agents, and ancillary imaging features. Radiology 273:30–50
15. Omata M, Cheng AL, Kokudo N et al (2017) Asia-Pacific clinical practice guidelines on the management of hepatocellular carcinoma: a 2017 update. Hepatol Int 11:317–370
16. Chernyak V, Fowler KJ, Kamaya A et al (2018) Liver Imaging Reporting and Data System (LI-RADS) version 2018: imaging of hepatocellular carcinoma in at-risk patients. Radiology 289:816–830
17. Park MJ, Kim YK, Lee MW et al (2012) Small hepatocellular carcinomas: improved sensitivity by combining gadoxetic acid-enhanced and diffusion-weighted MR imaging patterns. Radiology 264:761–770
18. Kim YK, Kim CS, Han YM, Park G (2010) Detection of small hepatocellular carcinoma: can gadoxetic acid-enhanced magnetic resonance imaging replace combining gadopentetate dimeglumine-enhanced and superparamagnetic iron oxide-enhanced magnetic resonance imaging? Invest Radiol 45:740–746
19. Phongkitkarun S, Limsamutpetch K, Tannaphai P, Jatchavala J (2013) Added value of hepatobiliary phase gadoxetic acid-enhanced MRI for diagnosing hepatocellular carcinoma in high-risk patients. World J Gastroenterol 19:8357–8365
20. Joo I, Lee JM, Lee DH, Jeon JH, Han JK (2019) Retrospective validation of a new diagnostic criterion for hepatocellular carcinoma on gadoxetic acid-enhanced MRI: can hypointensity on the hepatobiliary phase be used as an alternative to washout with the aid of ancillary features? Eur Radiol 29:1724–1732
21. Renzulli M, Biselli M, Brocchi S et al (2018) New hallmark of hepatocellular carcinoma, early hepatocellular carcinoma and high-grade dysplastic nodules on Gd-EOB-DTPA MRI in patients with cirrhosis: a new diagnostic algorithm. Gut 67:1674–1682
22. Kim DH, Choi SH, Kim SY, Kim MJ, Lee SS, Byun JH (2019) Gadoxetic acid-enhanced MRI of hepatocellular carcinoma: value of washout in transitional and hepatobiliary phases. Radiology 291:651–657
23. McInnes MDF, Moher D, Thombs BD, McGrath TA, Bossuyt PM, Grp P-D (2018) Preferred Reporting Items for a Systematic Review and Meta-analysis of Diagnostic Test Accuracy Studies The PRISMA-DTA Statement. JAMA 319:388–396
24. Whiting PF, Rutjes AW, Westwood ME et al (2011) QUADAS-2: a revised tool for the quality assessment of diagnostic accuracy studies. Ann Intern Med 155:529–536

25. Higgins J, Green S Cochrane handbook for systematic reviews of interventions of interventions version 5.1.0. The Cochrane Collaboration. http://handbookcochraneorg/chapter_9/9_5_2_identifying_and_measuring_heterogeneityhtm Updated March 2011 Accessed May 28, 2015
26. Vogelgesang F, Schlattmann P, Dewey M (2018) The evaluation of bivariate mixed models in meta-analyses of diagnostic accuracy studies with SAS, Stata and R. Methods Inf Med 57:111–119
27. Doebler P, Holling H, Bohning D (2012) A mixed model approach to meta-analysis of diagnostic studies with binary test outcome. Psychol Methods 17:418–436
28. Deeks JJ, Macaskill P, Irwig L (2005) The performance of tests of publication bias and other sample size effects in systematic reviews of diagnostic test accuracy was assessed. J Clin Epidemiol 58:882–893
29. Choi SH, Byun JH, Lim YS et al (2016) Diagnostic criteria for hepatocellular carcinoma ≤ 3 cm with hepatocyte-specific contrast-enhanced magnetic resonance imaging. J Hepatol 64:1099–1107
30. Di Pietropaolo M, Briani C, Federici GF et al (2015) Comparison of diffusion-weighted imaging and gadoxetic acid-enhanced MR images in the evaluation of hepatocellular carcinoma and hypovascular hepatocellular nodules. Clin Imaging 39:468–475
31. Zhao XT, Li WX, Chai WM, Chen KM (2014) Detection of small hepatocellular carcinoma using gadoxetic acid-enhanced MRI: Is the addition of diffusion-weighted MRI at 3.0T beneficial? J Dig Dis 15:137–145
32. Park MJ, Kim YK, Lee MH, Lee J (2013) Validation of diagnostic criteria using gadoxetic acid-enhanced and diffusion-weighted MR imaging for small hepatocellular carcinoma (<= 2.0 cm) in patients with hepatitis-induced liver cirrhosis. Acta Radiol 54:127–136
33. Granito A, Galassi M, Piscaglia F et al (2013) Impact of gadoxetic acid (Gd-EOB-DTPA)-enhanced magnetic resonance on the non-invasive diagnosis of small hepatocellular carcinoma: a prospective study. Aliment Pharmacol Ther 37:355–363
34. Golfieri R, Renzulli M, Lucidi V, Corcioni B, Trevisani F, Bolondi L (2011) Contribution of the hepatobiliary phase of Gd-EOB-DTPA-enhanced MRI to Dynamic MRI in the detection of hypovascular small (< = 2 cm) HCC in cirrhosis. Eur Radiol 21:1233–1242
35. Paisant A, Vilgrain V, Riou J et al (2020) Comparison of extracellular and hepatobiliary MR contrast agents for the diagnosis of small HCCs. J Hepatol 72:937–945
36. Zhou Y, Jing X, Zhang X et al (2019) Combining the arterial phase of contrast-enhanced ultrasonography, gadoxetic acid-enhanced magnetic resonance imaging and diffusion-weighted imaging in the diagnosis of hepatic nodules ≤ 20 mm in patients with cirrhosis. Ultrasound Med Biol 45:693–701
37. Joo I, Lee JM, Lee DH, Jeon JH, Han JK, Choi BI (2015) Noninvasive diagnosis of hepatocellular carcinoma on gadoxetic acid-enhanced MRI: can hypointensity on the hepatobiliary phase be used as an alternative to washout? Eur Radiol 25:2859–2868
38. Kim YK, Kim YK, Park HJ, Park MJ, Lee WJ, Choi D (2014) Noncontrast MRI with diffusion-weighted imaging as the sole imaging modality for detecting liver malignancy in patients with high risk for hepatocellular carcinoma. Magn Reson Imaging 32:610–618
39. Kim MY, Kim YK, Park HJ, Park MJ, Lee WJ, Choi D (2014) Diagnosis of focal liver lesions with gadoxetic acid-enhanced MRI: is a shortened delay time possible by adding diffusion-weighted imaging? J Magnc Reson Imaging 39:31–41
40. Hwang J, Kim YK, Kim JM, Lee WJ, Choi D, Hong SS (2014) Pretransplant diagnosis of hepatocellular carcinoma by gadoxetic acid-enhanced and diffusion-weighted magnetic resonance imaging. Liver Transpl 20:1436–1446
41. Kim YK, Kim CS, Han YM, Lee YH (2011) Detection of liver malignancy with gadoxetic acid-enhanced MRI: is addition of diffusion-weighted MRI beneficial? Clin Radiol 66:489–496
42. Chou CT, Chen YL, Su WW, Wu HK, Chen RC (2010) Characterization of cirrhotic nodules with gadoxetic acid-enhanced magnetic resonance imaging: the efficacy of hepatocyte-phase imaging. J Magnc Reson Imaging 32:895–902
43. Choi MH, Choi JI, Lee YJ, Park MY, Rha SE, Lall C (2017) MRI of small hepatocellular carcinoma: typical features are less frequent below a size cutoff of 1.5 cm. AJR Am J Roentgenol 208:544–551
44. Yu MH, Kim JH, Yoon JH et al (2014) Small (< = 1-cm) Hepatocellular carcinoma: diagnostic performance and imaging features at gadoxetic acid-enhanced MR imaging. Radiology 271:748–760
45. Park VY, Choi JY, Chung YE et al (2014) Dynamic enhancement pattern of HCC smaller than 3 cm in diameter on gadoxetic acid-enhanced MRI: comparison with multiphasic MDCT. Liver Int 34:1593–1602
46. Ooka Y, Kanai F, Okabe S et al (2013) Gadoxetic acid-enhanced MRI compared with CT during angiography in the diagnosis of hepatocellular carcinoma. Magn Reson Imaging 31:748–754
47. Choi JW, Lee JM, Kim SJ et al (2013) Hepatocellular carcinoma: imaging patterns on gadoxetic acid-enhanced MR images and their value as an imaging biomarker. Radiology 267:776–786
48. Rhee H, Kim MJ, Park YN, Choi JS, Kim KS (2012) Gadoxetic acid-enhanced MRI findings of early hepatocellular carcinoma as defined by new histologic criteria. J Magnc Reson Imaging 35:393–398
49. Rhee H, Kim MJ, Park MS, Kim KA (2012) Differentiation of early hepatocellular carcinoma from benign hepatocellular nodules on gadoxetic acid-enhanced MRI. Br J Radiol 85:e837–e844
50. Kim AY, Kim YK, Lee MW et al (2012) Detection of hepatocellular carcinoma in gadoxetic acid-enhanced MRI and diffusion-weighted MRI with respect to the severity of liver cirrhosis. Acta Radiol 53:830–838
51. Kim YK, Kim CS, Han YM, Yu HC, Choi D (2011) Detection of small hepatocellular carcinoma: intraindividual comparison of gadoxetic acid-enhanced MRI at 3.0 and 1.5 T. Invest Radiol 46:383–389
52. Kawada N, Ohkawa K, Tanaka S et al (2010) Improved diagnosis of well-differentiated hepatocellular carcinoma with gadolinium ethoxybenzyl diethylene triamine pentaacetic acid-enhanced magnetic resonance imaging and Sonazoid contrast-enhanced ultrasonography. Hepatol Res 40:930–936
53. Di Martino M, Marin D, Guerrisi A et al (2010) Intraindividual comparison of gadoxetate disodium-enhanced MR imaging and 64-section multidetector CT in the detection of hepatocellular carcinoma in patients with cirrhosis. Radiology 256:806–816
54. Kierans AS, Kang SK, Rosenkrantz AB (2016) The diagnostic performance of dynamic contrast-enhanced MR imaging for detection of small hepatocellular carcinoma measuring up to 2 cm: a meta-analysis. Radiology 278:82–94
55. Lee YJ, Lee JM, Lee JS et al (2015) Hepatocellular carcinoma: diagnostic performance of multidetector CT and MR imaging-a systematic review and meta-analysis. Radiology 275:97–109
56. Mazzaferro V, Llovet JM, Miceli R et al (2009) Predicting survival after liver transplantation in patients with hepatocellular carcinoma beyond the Milan criteria: a retrospective, exploratory analysis. Lancet Oncol 10:35–43
57. Bashir MR, Gupta RT, Davenport MS et al (2013) Hepatocellular carcinoma in a North American population: does hepatobiliary MR imaging with Gd-EOB-DTPA improve sensitivity and confidence for diagnosis? J Magn Reson Imaging 37:398–406

58. Palmucci S (2014) Focal liver lesions detection and characterization: the advantages of gadoxetic acid-enhanced liver MRI. World J Hepatol 6:477–485
59. Deeks JJ (2001) Systematic reviews in health care - systematic reviews of evaluations of diagnostic and screening. BMJ 323: 157–162
60. Gregoire G, Derderian F, Le Lorier J (1995) Selecting the language of the publications included in a meta-analysis: is there a Tower of Babel bias? J Clin Epidemiol 48:159–163